Development 104, 285–295 (1988)
Printed in Great Britain © The Company of Biologists Limited 1988

A cell-type-specific abnormality of cell proliferation in mutant (curly tail) mouse embryos developing spinal neural tube defects

ANDREW J. COPP[1], FRANCES A. BROOK[1] and HEATHER J. ROBERTS[2]

[1]*Imperial Cancer Research Fund, Developmental Biology Unit, Department of Zoology, University of Oxford, South Parks Road, Oxford OX1 3PS, UK*
[2]*Paediatric Research Unit, The Prince Philip Research Laboratories, Guy's Hospital, London SE1 9RT, UK*

Summary

The mouse mutant curly tail (*ct*) provides a model system for studies of neurulation mechanisms. 60 % of *ct/ct* embryos develop spinal neural tube defects (NTD) as a result of delayed neurulation at the posterior neuropore whereas the remaining 40 % of embryos develop normally. In order to investigate the role of cell proliferation during mouse neurulation, cell cycle parameters were studied in curly tail embryos developing spinal NTD and in their normally developing litter-mates. Measurements were made of mitotic index, median length of S-phase and percent reduction of labelling index during a [^{3}H]thymidine pulse-chase experiment. These independent measures of cell proliferation rate indicate a reduced rate of proliferation of gut endoderm and notochord cells in the neuropore region of embryos developing spinal NTD compared with normally developing controls. The incidence of cell death and the relative frequency of mitotic spindle orientations does not differ consistently between normal and abnormal embryos. These results suggest a mechanism of spinal NTD pathogenesis in curly tail embryos based on failure of normal cell proliferation in gut endoderm and notochord.

Key words: cell proliferation, mutant, mouse, embryo, neural tube defects, spinal neural tube.

Introduction

A role for cell proliferation in the mechanism of vertebrate neurulation was suggested over a century ago (His, 1874). More recent studies have demonstrated that neurulation in mammals and birds is correlated with rapid embryonic cell proliferation (Jelinek & Friebova, 1966; Kauffman, 1968; Wilson, 1982), whereas amphibian embryos undergo neurulation without appreciable increase in cell number (Gilette, 1944). Thus, cell proliferation may play a role in the mechanism of neurulation in higher vertebrates.

Experimental evidence pertaining to the role of cell proliferation in mammalian and avian neurulation has come from studies of embryos undergoing abnormal neurulation due to environmental or genetic influences. Several agents, e.g. urethane (Kauffman, 1969), insulin (Cole & Trasler, 1980) and bromodeoxyuridine (Bannigan, 1985) interfere with neurulation and also produce a lengthening of the neuroepithelial cell cycle. Moreover, mouse embryos homozygous for the mutations Splotch and Looptail have a lengthened neuroepithelial cell cycle in regions of open cranial NTD by comparison with normal embryos that have completed neurulation (Wilson, 1974; Wilson & Center, 1974). A similar disturbance of the cell cycle probably also occurs in human embryos with spontaneous NTD (Patten, 1953; Wilson, 1980).

A limitation of these previous studies is that environmental and genetic effects on embryonic cell proliferation have usually been evaluated relatively late in the development of NTD when neurulation is complete in normal control embryos and abnormal embryos can be easily recognized. This raises the possibility that abnormalities of cell proliferation observed in the studies may have arisen as a consequence of abnormal morphogenesis and do not reflect the aberrant cell behaviour that led originally to defective neurulation. In this context, it is interesting to note that studies of cell proliferation in Trypan Blue-induced spina bifida, in which embryos were analysed early in the process of abnormal morpho-

genesis, did not reveal a disturbance of the embryonic cell cycle (Lendon, 1972; Peters & De Geus, 1981).

A further limitation of previous studies is that they have been concerned primarily with the neuroepithelial cell cycle. Analysis of cell proliferation in other cell types has been performed in only a few cases (Atlas & Bond, 1965; Lendon, 1972; Smith & Schoenwolf, 1987).

In an attempt to overcome these shortcomings, we asked whether proliferation of any of the five resident cell types constituting the lower spinal region of the mouse embryo is disturbed during the earliest stages of development of spinal NTD. We studied mouse embryos homozygous for the curly tail mutation (*ct*) that develop spinal NTD as a result of delayed neurulation at the posterior neuropore (Copp, 1985). The incomplete penetrance of the curly tail mutation (Gruneberg, 1954) means that single litters of homozygous embryos contain both individuals developing normally and those developing spinal NTD. In the present study, we utilized a morphological 'marker' (Copp, 1985) to distinguish embryos developing spinal NTD from their normally developing littermates prior to the normal time that neurulation is completed.

Three independent methods (mitotic index, length of S-phase and percent reduction in labelling index during [^{3}H]thymidine pulse-chase) were used to compare cell proliferation rates in normal and abnormal curly tail embryos. *Mitotic index* provided the primary basis of comparison. Measurements were made of the percentage of cells in mitosis at the time of fixation of embryos, without the use of stathmokinetic agents. Accurate estimates of cell proliferation rates from mitotic index measurements require that allowance is made for differences between cell populations in the proportion of cells progressing around the cell cycle (i.e. the growth fraction). For this reason, *growth fraction* was also measured using continuous labelling with [^{3}H]thymidine.

Percent labelled mitoses (PLM)–time curves were constructed from [^{3}H]thymidine pulse-chase experiments in order to determine the median *length of S-phase*. Statistical comparison of measurements derived from different PLM–time curves is problematical (Wright & Alison, 1984). Hence, values of S-phase length were used primarily to corroborate the findings of the mitotic index analysis.

Percent reduction in labelling index, a measure of the rate of appearance of unlabelled cells, was determined for a [^{3}H]thymidine 2 h pulse–12 h chase experiment as a further measure of the mean rate of cell proliferation. Loss of cells during the chase period due to cell death can introduce inaccuracies into the estimation of cell proliferation rate based on reduction in labelling index (Wright & Alison, 1984). For this reason, the incidence of *cell death* was determined for all cell types in the study.

Differences between cell types in the *relative orientation of mitotic spindles* may affect the pattern of tissue growth in the absence of variations in cell proliferation rates. Thus, the relative abundance of mitotic spindles oriented parallel and perpendicular to the long axis of the embryo was measured for all cell types.

Materials and methods

Curly tail mice

The curly tail (*ct*) mutation was established on the CBA/Gr genetic background (Gruneberg, 1954). The curly tail stock is now maintained as a closed, random-bred colony of homozygous *ct/ct* mice. Spinal NTD develop in approximately 60 % of homozygotes: two-thirds of the abnormal mice have tail flexion defects (i.e. curly tails) and one-third have open lumbosacral spina bifida with tail flexion defects (Embury *et al.* 1979; Copp *et al.* 1982). The remaining 40 % of *ct/ct* mice are morphologically normal. Experimental litters were obtained from matings between affected males and either affected or unaffected females (all *ct/ct*). Mice were maintained on a light cycle with dark period 7.00 p.m. to 7.00 a.m. Males were paired with females for mating either overnight, in which case females were checked for copulation plugs the following morning, or between 8.00 and 9.00 a.m. when females were checked for plugs 6–8 h later. The day of finding a copulation plug was designated day 1 of gestation.

Embryos were harvested for analysis, in both *in vivo* and *in vitro* experiments, on day 11 of gestation when they had 27–29 somites. At this stage, embryos developing spinal NTD can be distinguished from their normally developing littermates on the basis of their abnormally enlarged posterior neuropores (Copp, 1985). Embryos from overnight matings reached the 27- to 29-somite stage between 6.00 and 9.00 a.m. on day 11, whereas embryos from morning matings reached the same stage between 11.00 a.m. and 2.00 p.m. on day 11.

[^{3}H]thymidine labelling in vivo

Pregnant females were given a single intraperitoneal injection of 5 μCi g^{-1} body weight [^{3}H]thymidine (2 Ci mmol^{-1}, diluted in 10 mM-phosphate-buffered saline, pH 7·4, PBS) at 1, 2, 3, 4, 5, 6, 7, 8, 10, 12 or 14 h prior to harvesting embryos. Some additional embryos were obtained from pregnant females that did not receive an injection of [^{3}H]thymidine. Conceptuses were explanted into prewarmed alpha-modification of Eagle's Minimal Essential Medium (Flow Labs, UK) containing 2 mM-glutamine, 20 mM-Hepes, 100 i.u. ml^{-1} penicillin, 100 μg ml^{-1} streptomycin and 10 % fetal calf serum (referred to later as α-MEM). Extraembryonic membranes were removed, embryos were washed several times in cold PBS and were fixed in Bouin's fluid at room temperature for at least 24 h.

[^{3}H]thymidine labelling in vitro

Conceptuses were explanted from pregnant females between 3.00 and 5.00 p.m. on day 9 of gestation. Ectoplacental cone, trophoblast giant cells, parietal endoderm and Reichert's membrane were removed whereas yolk sac, chorion and amnion were maintained intact. Embryos were allowed to recover in culture (method of New *et al.* 1973) for at least 2 h before being labelled by culture for a further 12 h in medium containing 1 μCi ml^{-1} [^{3}H]thymidine (2 Ci mmol^{-1}). After labelling, extraembryonic membranes were removed in ice-cold α-MEM, embryos were washed in several changes of PBS and fixed in Bouin's fluid.

Assessment of somite number and neuropore category

Somites were counted following fixation of embryos as described previously (Copp *et al.* 1982). Embryos with 27 to 29 somites were selected for analysis and were grouped according to posterior neuropore category. The following neuropore categories have been defined for curly tail embryos with 27 to 29 somites (Copp, 1985). Category 1/2 embryos (small neuropores) develop normally in more than 60 % of cases, the remainder developing tail flexion defects (i.e. curly tails). Category 3 embryos (moderately enlarged neuropores) develop normally in 30 % of cases with 70 % of embryos developing tail flexion defects. A small minority of these abnormal embryos also have open lumbosacral spina bifida. Less than 10 % of category 4/5 embryos (severely enlarged neuropores) develop normally. The remainder develop spinal NTD comprising tail flexion defects with open spina bifida in 15–30 % of cases. Curly tail embryos with 27–29 somites are distributed approximately equally between the three neuropore categories. In the present experiments, only embryos in categories 1/2 and 4/5 were analysed, those in category 3 being discarded.

Preparation of embryos for cell proliferation analysis

Posterior regions of fixed embryos, isolated by a cut at approximately the level of somite 20, were dehydrated through graded alcohols, embedded in paraffin wax (m.p. 56°C) and prepared as serial transverse sections, thickness 6 μm. Sections of embryos labelled with [^{3}H]thymidine were rehydrated, treated with 5 % trichloroacetic acid for 30 min at 4°C and then exposed to autoradiographic stripping film (Kodak AR10). Length of exposure was determined separately for each batch of autoradiograms by examining test slides developed at intervals following exposure to emulsion. Sections of embryos labelled *in vivo* were exposed for 2–4 weeks and sections of embryos labelled *in vitro* were exposed for 4–8 days. In each experiment, category 1/2 and 4/5 embryos to be compared were subjected to identical periods of autoradiographic exposure. After developing, autoradiograms were counterstained with Mayer's or Harris's haematoxylin.

Embryos removed from pregnant females without prior labelling were fixed, embedded and sectioned as described above. Sections were stained with haematoxylin and eosin.

Embryonic regions analysed

Embryos were analysed at two sites along the neuraxis (Fig. 1). The 'distal' site contained sections through the region of active neural fold elevation in category 1/2 embryos and through a region of relatively flat neural folds in category 4/5 embryos. The 'proximal' site contained sections through the region of active neural fold elevation in

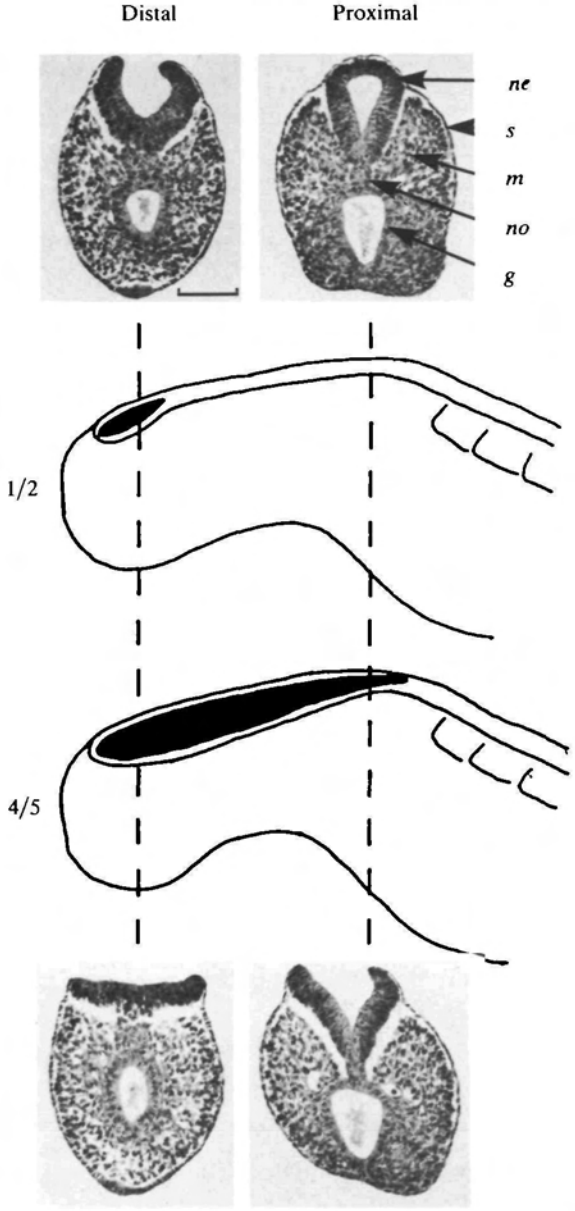

Fig. 1. Diagrams and photomicrographs illustrating the method used to compare cell proliferation rates between normal (category 1/2, upper diagram and sections) and abnormal (category 4/5, lower diagram and sections) curly tail embryos. Transverse histological sections were obtained from 'proximal' and 'distal' sites. Proximal sections contained, in category 1/2 embryos, a region of closed neural tube and, in category 4/5 embryos, the cranial extremity of the enlarged posterior neuropore, the site of active neurulation. Distal sections contained, in category 1/2 embryos, the cranial end of the normal-sized neuropore, the site of active neurulation and, in category 4/5 embryos, a region of relatively flat neural plate in the caudal part of the enlarged neuropore. Cell types studied: *ne*, neuroepithelium; *s*, surface ectoderm; *m*, mesoderm; *no*, notochord; *g*, gut endoderm. Bar, 100 μm.

category 4/5 embryos and through a region of closed neural tube in category 1/2 embryos. Preliminary experiments using three-dimensional reconstruction of serial sections showed that individual cells rarely occupy more than two consecutive 6 μm sections. Therefore, data were collected from alternate serial 6 μm sections. A block of six alternate sections (spanning 72 μm of embryo length) was analysed at both proximal and distal sites. Throughout the study, embryos were coded and analysed 'blind' with regard to embryonic region and neuropore category.

Cell counts and analysis of autoradiograms

Mitoses (i.e. metaphase and anaphase figures) were counted for each of the five cell types under study (see Fig. 1). The orientation of mitotic spindles was recorded as parallel or perpendicular to the plane of section or, in cases of doubt, as unknown. Dead cells, counted only in sections stained with haematoxylin and eosin, were recognized by criteria described previously (Copp, 1978). Total nuclear count (including interphase nuclei and mitoses but excluding dead cells) was made on a single section located midway through each block of sections. An estimate of the total number of cells in the block of scored sections was obtained by multiplying this nuclear count by the number of sections analysed in the block (assuming all cells to be uninucleate).

Background labelling in autoradiograms was determined separately for each block of sections by counting grains over known areas, defined by an eyepiece graticule, adjacent to a section located midway through the block. This grain count, divided by the mean number of neuroepithelial nuclei found to fit within the area measured, gave the mean nuclear background count. Nuclei and mitotic figures were considered labelled if they had more than the background grain count. Embryos with background counts exceeding four grains per nucleus were excluded from the analysis.

Calculation of cell cycle parameters

1. Mitotic index (MI) =

$$\frac{\text{Number of mitoses}}{\text{Total number of viable cells}} \times 100$$

Mitotic indices were obtained by counting all mitoses (and estimating total cell number, as described above) in blocks of six sections at each proximal and distal embryonic site (see Fig. 1). Since the five cell types under study occur in the embryo in differing numbers, a different number of mitoses was counted for each cell type in each individual embryo region. Numbers of mitoses scored per individual embryo region (averaged across all embryo categories) were as follows: mesoderm, 53; neuroepithelium, 32; gut endoderm, 11; surface ectoderm, 9; notochord, 2. As expected, interembryo variability (measured as the standard deviation of MI values as a percentage of mean MI) was greatest for notochord where fewest mitoses were scored and least for mesoderm (data not shown). In order to permit meaningful statistical analysis, data values from replicate embryos were pooled to yield a single MI value for each combination of embryo category, embryo region and cell type (see Table 1 for pooled MI values). The MI analysis was performed on two seperate groups of embryos in order to provide an estimate of interexperiment variability (see Fig. 2).

2. Growth fraction (from continuous labelling experiment)

$$= \frac{\text{Number of labelled nuclei}}{\text{Total nuclear number}} \times 100$$

3. Percent labelled mitoses (PLM, from pulse-chase experiment)

$$= \frac{\text{Number of labelled mitoses}}{\text{Total number of mitoses}} \times 100$$

Pooled values for PLM were obtained from between two and five embryos at each time point, for each combination of embryo category, embryo region and cell type as described for MI values. Median length of S-phase was measured from the time interval between 50% points on the ascending and descending limbs of the PLM–time curve.

4. Percent reduction in labelling index (during pulse-chase experiment)

$$= \frac{[\text{labelling index after pulse}] - [\text{labelling index after chase}]}{\text{labelling index after pulse}} \times 100$$

5. Dead cell index $= \frac{\text{Number of dead cells}}{\text{Total number of viable cells}} \times 100$

Statistical analysis

Comparisons were made for each cell type between embryo regions using chi-squared 'comparisons of two proportions' tests. In cases where single data values were used in multiple comparisons (e.g. Table 1, Fig. 5), the Bonferroni correction (Glantz, 1981) was applied by increasing the value of P corresponding to a given χ^2 value by a factor equal to the number of tests in which the data value was used.

Results

Cell proliferation parameters were compared between proximal and distal regions of category 1/2 and 4/5 embryos (Fig. 1). Of the six possible pairwise comparisons, the following three were considered to be most informative and, therefore, formed the basis of the analysis:

(a) 1/2 proximal *versus* 1/2 distal. A comparison providing information on the variation of cell proliferation parameters between regions of closed neural tube and active neurulation in normally developing embryos.

(b) 1/2 distal *versus* 4/5 proximal. A comparison of sites of active neurulation in normally and abnormally developing embryos, not matched for neuraxial level.

(c) 1/2 distal *versus* 4/5 distal. A comparison of regions of normal and abnormal embryos matched for neuraxial level but differing in the degree to which neurulation had progressed.

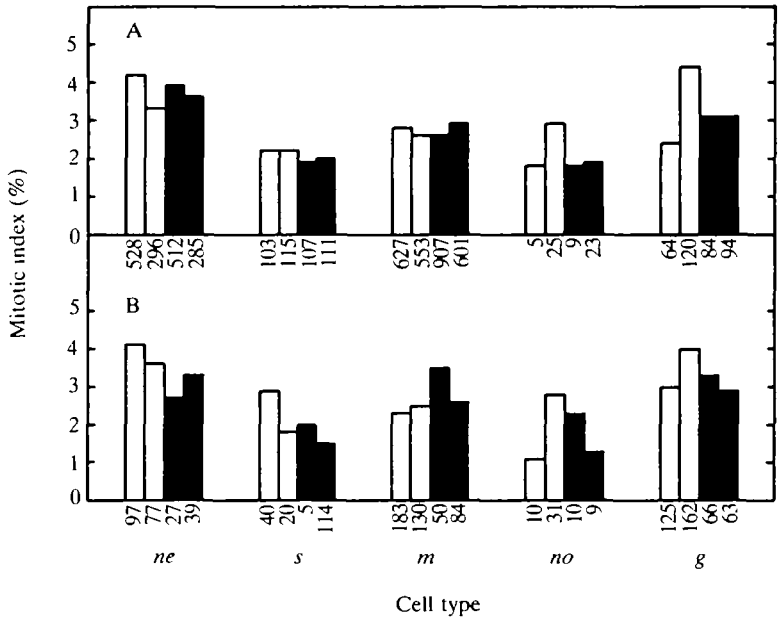

Fig. 2. Mitotic indices in curly tail embryos determined from two independent experiments (A,B). Open bars represent category 1/2 embryos and solid bars represent category 4/5 embryos. The left bar represents proximal, and the right bar distal, embryonic sites in each pair. Twelve embryos of each category were analysed in experiment A and thirteen embryos of each category in experiment B. Figures beneath bars show the number of mitoses scored. Mitotic indices calculated as in Materials and methods. Abbreviations of cell types: see Fig. 1. Statistical analysis: see Table 1.

Table 1. *Comparison of mitotic indices between category 1/2 and 4/5 embryos*

	Category 1/2		Category 4/5	
Cell type	Proximal	Distal	Proximal	Distal
Neuroepithelium	4·2*,†	3·4†	3·8	3·5*
Surface ectoderm	2·4	2·1	1·9	2·0
Mesoderm	2·6	2·5	2·7	2·8
Notochord	1·3*	2·8*	2·0	1·7
Gut endoderm	2·8‡	4·2*,†,‡	3·1*	3·1†

Mitotic indices are pooled values for each combination of embryo category, embryo region and cell type.

Pair-wise χ^2 comparisons were performed within each row of the table. Paired MI values sharing a superscript differ significantly from each other with the following *P* values (after application of Bonferroni's correction):

* < 0·05
† < 0·01
‡ < 0·005.

Mitotic index (MI)

(a) *Comparisons within embryo categories*

MI values differed significantly between proximal and distal sites of category 1/2 embryos in neuroepithelium, notochord and gut endoderm, but not in surface ectoderm and mesoderm (Fig. 2; Table 1). Neuroepithelial values were significantly greater at proximal than distal sites whereas notochord and gut endoderm MI showed the opposite trend: values at the distal site significantly exceeded those at the proximal site. Proximal/distal comparisons for category 4/5 embryos yielded nonsignificant differences for all cell types (Fig. 2; Table 1).

(b) *Comparisons between embryo categories*

Gut endoderm of both proximal and distal sites of category 4/5 embryos exhibited significantly lower MI values than the distal site of category 1/2. Other cell types showed no significant differences in this comparison although notochordal values were reduced consistently at both proximal and distal sites in category 4/5 embryos compared with the distal site of category 1/2 embryos. Failure of these differences to reach statistical significance perhaps reflects the small number of cells available for scoring in the notochord (see Materials & Methods).

Growth fraction

Growth fraction was measured by determining the labelling index of cells following continuous exposure of embryos to [^{3}H]thymidine for 12 h *in vitro* (a period in excess of the probable cell cycle length; see Conclusion section later). Notochord in distal embryonic sites was the only cell type with a growth fraction of less than 95%, a finding that applied equally to category 1/2 and 4/5 embryos (Table 2). It is possible that a G_0 cell subpopulation exists in the notochord. Alternatively, the length of the cell cycle may be especially variable in the notochord so that the most slowly cycling cells (approximately 10%) did not undergo DNA replication during the 12 h labelling period. The consistently high values recorded for other cell types suggest that, in these cases, the entire cell populations are progressing around the cell cycle.

PLM–time curves

[^{3}H]thymidine pulse-chase experiments were performed *in vivo* in order to follow the time course of a cohort of labelled cells through the cell cycle. Median length of S-phase (determined from PLM–time curves) was shortest in neuroepithelium of all embryo categories and regions (Fig. 3A,C,E,G) and in gut endoderm of category 1/2 embryos (Fig. 4B,D).

Table 2. *Growth fraction of cell types in curly tail embryos*

	Category 1/2		Category 4/5	
Cell type	Proximal	Distal	Proximal	Distal
Neuro-epithelium	99·6 ± 0·2*	99·3 ± 0·5	99·8 ± 0·2	100·0 ± 0
Surface ectoderm	96·2 ± 0·8	96·0 ± 1·6	95·2 ± 2·4	97·0 ± 0·2
Mesoderm	98·7 ± 1·3	99·7 ± 0·4	99·8 ± 0·2	99·8 ± 0·2
Notochord	96·1 ± 3·9	89·1 ± 4·5	94·5 ± 3·8	92·7 ± 3·8
Gut endoderm	95·8 ± 1·2	98·6 ± 0·6	97·7 ± 1·8	99·5 ± 0·3

* Mean ± standard error of the mean, observations on three embryos in each case.

Statistical analysis: pairwise comparisons (1/2 proximal *vs* 1/2 distal; 1/2 distal *vs* 4/5 proximal; 1/2 distal *vs* 4/5 distal) using *t*-tests with Bonferroni correction of three nonindependent comparisons yielded no significant differences for any cell type.

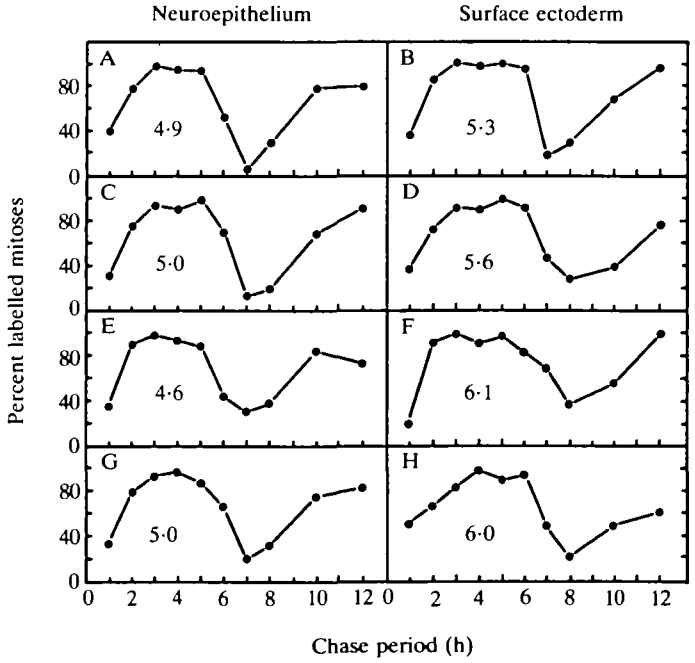

Fig. 3. Percent labelled mitoses in curly tail embryos during a [^{3}H]thymidine pulse-chase experiment. From top to bottom, graphs represent: category 1/2 proximal site (A,B); category 1/2 distal site (C,D); category 4/5 proximal site (E,F); category 4/5 distal site (G,H). Left-side graphs (A,C,E,G) represent neuroepithelium, right-side graphs (B,D,F,H) represent surface ectoderm. Figures beneath the PLM peak show median lengths of S-phase measured as the time interval between 50% points on ascending and descending limbs of the peak. Mean number of mitoses scored per time point (averaged across all embryo categories and sites) were as follows: neuroepithelium, 109; surface ectoderm, 29.

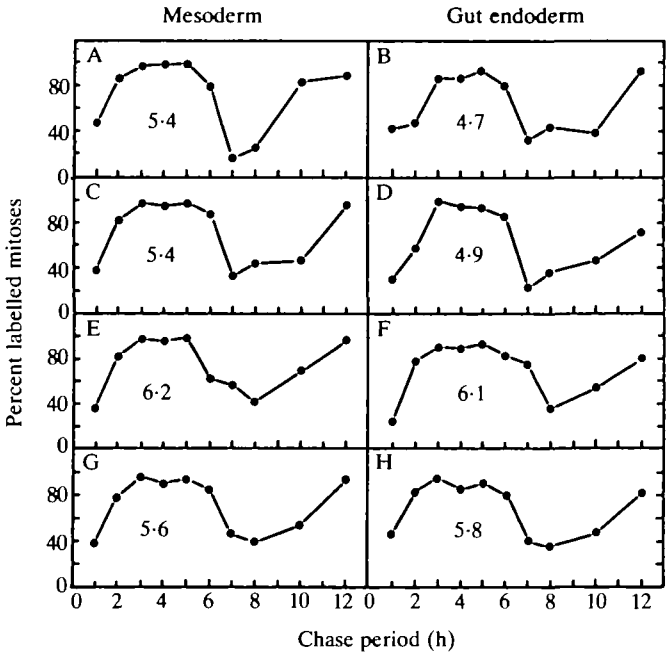

Fig. 4. Percent labelled mitoses in curly tail embryos during a [^{3}H]thymidine pulse-chase experiment. Details as for Fig. 3 except that left-side graphs (A,C,E,G) represent mesoderm and right-side graphs (B,D,F,H) represent gut endoderm. Mean numbers of mitoses scored per time point (averaged across all embryo categories and sites) were as follows: mesoderm, 199; gut endoderm, 35.

These cell types also had the largest MI values (Fig. 2, Table 1) indicating that their proliferation is indeed most rapid.

Differences in S-phase length between category 1/2 and 4/5 embryos were most marked for gut endoderm: category 1/2 embryos exhibited markedly lower values than category 4/5 embryos (Fig. 4 compare B,D with F,H). Differences between category 1/2 and 4/5 embryos also occurred in surface ectoderm (Fig. 3 compare B,D with F,H) and in mesoderm (Fig. 4 compare A,C,G with E) but these differences were of smaller magnitude than observed for gut endoderm. Numbers of mitoses collected for notochord were too small to permit construction of curves for this cell type.

Percent reduction in labelling index during a pulse-chase experiment

Labelling index was determined for neuroepithelium, mesoderm, notochord and gut endoderm of embryos collected 2 h and 14 h after a single injection of [^{3}H]thymidine into pregnant females. Neuroepithelium and mesoderm showed no significant differences between category 1/2 and 4/5 embryos in percent reduction of labelling index following the chase period (Fig. 5). By contrast, notochord and gut endoderm showed a significantly smaller reduction in

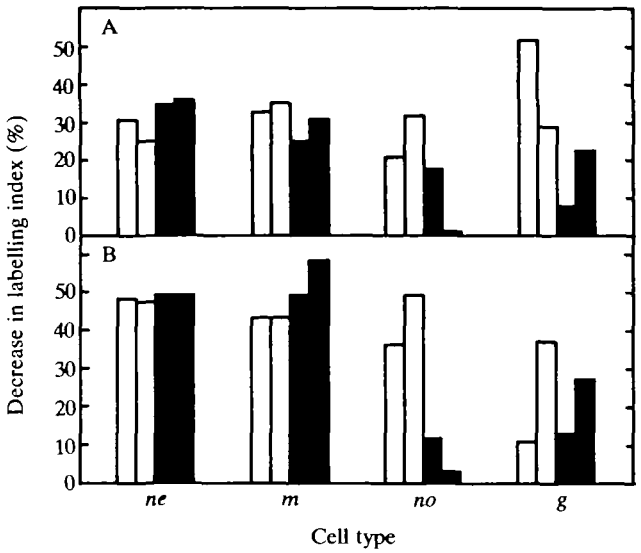

Fig. 5. Percent reduction in labelling index in curly tail embryos determined from two independent [^{3}H]thymidine pulse-chase experiments (A,B). Open bars represent category 1/2 embryos and solid bars represent category 4/5 embryos. Each pair of adjacent bars represents proximal (left-sided bar) and distal (right-sided bar) embryonic sites for a given combination of embryo category and cell type. Percent reduction in labelling index calculated as in Materials and methods. Abbreviations of cell types: see Fig. 1. Statistical analysis: pairwise comparisons yielded significant differences (χ^2 comparison of two proportions, Bonferroni correction for three nonindependent tests, $P < 0{\cdot}05$) as follows: (i) 1/2 proximal *vs* 1/2 distal: gut endoderm both experiments, but *n.b.* with opposite signs of χ^2. (ii) 1/2 distal *vs* 4/5 proximal: notochord experiment B, gut endoderm both experiments. (iii) 1/2 distal *vs* 4/5 distal: notochord both experiments.

labelling index in category 4/5 embryos by comparison with the distal site of category 1/2 embryos. This difference from category 1/2 was most marked, for the notochord, in the distal site of category 4/5 embryos and, for the gut endoderm, in the proximal site of category 4/5 embryos. Values for the proximal site of category 1/2 embryos were, for unknown reasons, highly variable.

Cell death

The frequency of cell death was greatest in gut endoderm (5–6 %) and notochord (1–2·5 %) whereas dead cells comprised less than 1 % of the cell population in other cell types (Table 3). Dead cell indices differed significantly between category 1/2 and 4/5 embryos only for neuroepithelium and mesoderm: a finding of uncertain importance considering the low level of cell death in these cell types.

Orientation of mitotic spindles

Mitotic spindles were oriented parallel to the long axis of the embryo with a consistently higher frequency in neuroepithelium than in other cell types (Table 4). The relative abundance of parallel and perpendicular spindle orientations differed significantly only for mesoderm in comparisons between category 1/2 and 4/5 embryos.

Table 3. *Dead cell indices in curly tail embryos*

	Category 1/2 ($n = 5$)		Category 4/5 ($n = 6$)	
Cell type	D/T	DI	D/T	DI
Neuroepithelium	7	0·23	39	0·79
	2983		4944	
Surface ectoderm	1	0·04	6	0·15
	2663		4014	
Mesoderm*	72	0·70	112	0·42
	10260		26541	
Notochord	11	2·30	3	1·10
	485		284	
Gut endoderm	76	5·53	128	5·58
	1374		2295	

Comparison was made between distal position of category 1/2 and proximal position of category 4/5 embryos in order to sample the sites of active neurulation in each embryo type.

Abbreviations: D, number of dead cells; T, number of viable cells; DI, dead cell index.

Statistical analysis: comparison between category 1/2 and 4/5 embryos yielded significant differences in the proportion of dead cells for neuroepithelium and mesoderm (χ^2 comparisons of two proportions, $P < 0{\cdot}005$).

Conclusion

The findings of the comparison between category 1/2 and 4/5 embryos are summarized in Table 5. The cell cycle length of an exponentially growing cell population can be calculated from the mitotic index according to the following formula:

$$t_g = \ln 2 \times t_m / MI$$

where t_g is the cell cycle length, ln2 is a factor compensating for exponential growth, t_m is the length of metaphase/anaphase, and MI is the mitotic index (Johnson, 1961; Steel, 1968). Assuming a length of metaphase/anaphase that does not differ between category 1/2 and 4/5 embryos and is equal to 0·5 h, the cell cycle length for 1/2 distal gut endoderm is 8·5 h and for 4/5 proximal and distal gut endoderm is 11·2 h. These values are consistent with the data from the PLM analysis (Fig. 4).

Discussion

The present study has identified a reduced rate of cell proliferation in gut endoderm and notochord of mutant curly tail embryos developing spinal NTD

Table 4. *Orientation of mitotic spindles in curly tail embryos*

	Category 1/2				Category 4/5			
		% cells				% cells		
Cell type	T	<>	*	?	T	<>	*	?
Neuroepithelium	106 (5)	45·3	32·1	22·6	177 (6)	46·3	43·5	10·2
Surface ectoderm	50 (5)	54·0	24·0	22·0	86 (6)	47·7	36·0	16·3
Mesoderm	250 (5)	61·6	24·4	14·0	582 (6)	56·9	33·5	9·6
Notochord	38 (14)	63·2	31·6	5·3	15 (14)	73·3	20·0	6·7
Gut endoderm	40 (5)	60·0	15·0	25·0	56 (6)	55·4	33·9	10·7

Comparison was made between distal position of category 1/2 and proximal position of category 4/5 embryos in order to sample the sites of active neurulation in each embryo type.

Abbreviations: T, total number of mitotic spindles scored; <>, spindles transverse to long axis of embryo; *, spindles parallel to long axis of embryo; ?, spindle orientation unknown. Values in parentheses indicate the number of embryos studied.

Statistical analysis: comparisons between category 1/2 and 4/5 embryos yielded significant differences in the relative abundance of <> and * orientations only for mesoderm (χ^2 2×2 contingency tables, $P<0{\cdot}05$).

Table 5. *Summary of differences in cell proliferation parameters between category 1/2 and 4/5 embryos*

Cell cycle parameter	Mitotic index	Median length of S-phase	% reduction in labelling index
Neuroepithelium	Larger in 1/2 prox. than in 4/5 dist.*	None	None
Surface ectoderm	None	Shorter in 1/2 than in 4/5	ND†
Mesoderm	None	Shorter in 1/2 than in 4/5	None
Notochord	Larger in 1/2 dist. than 4/5 prox. and dist.	ND	Larger in 1/2 dist. than in 4/5*
Gut endoderm	Larger in 1/2 dist. than in 4/5*	Shorter in 1/2 than in 4/5	Larger in 1/2 dist. than in 4/5 prox.*

* Indicates differences that are statistically significant.
† ND: not determined.

compared with their normally developing littermates. Proliferation of other cell types appears unaffected in embryos developing spinal NTD. This conclusion is based on measurements of cell proliferation rate using several methods of analysis. Before discussing the developmental implications of these findings, it is important to consider some aspects of the cell cycle methodology used in the study.

Methodological considerations in the cell cycle analysis

The experimental analysis of cell cycle kinetics is an area of long-standing controversy (reviewed by Wright & Alison, 1984). Criticisms of previous studies have involved pinpointing the presence of false or untested assumptions that introduced errors into experimentally determined values of cell cycle parameters. The aim of the present study was not to obtain accurate numerical values for cell cycle parameters, but rather to perform a comparative analysis of cell proliferation rates between curly tail embryos developing normally and those developing spinal NTD. To this end, normal and abnormal embryos were labelled under identical conditions *in vivo* and *in vitro* and were analysed 'blind', by identical methods.

The study employed three independent analytical methods that examined different aspects of the cell cycle. This meant that differences between normal and abnormal embryos affecting specific phases of the cell cycle (such as the prolongation of mitosis described for the neuroepithelium of hindbrain NTD in homozygous Looptail embryos; Wilson, 1980) could be distinguished from differences in overall cell cycle length. Since the mutant phenotype in *ct/ct* embryos shows all possible degrees of severity, from mild tail kinks to open spina bifida, it seemed likely at the outset that the cellular and molecular defects in affected *ct/ct* embryos would be quantitative in nature. The use of multiple methods of analysis increased the likelihood that a relatively small quantitative difference between normal and abnormal *ct/ct* embryos in cell proliferation rate would be recognized. In practice, several apparent differences in cell cycle parameters were observed that were not corroborated by other methods of analysis (see Table 5). By contrast, the observed differences between normal and abnormal embryos in proliferation of gut endoderm and notochord cells were reproducible, using three and two methods, respectively, suggesting that normal and abnormal *ct/ct* embryos differ in overall rate of cell proliferation in these cell types.

Several specific assumptions of the cell cycle analytical methods employed were tested. Growth fractions were measured in order to determine whether differences in mitotic index may have arisen as a result of the presence in some cell populations of noncycling cells. Furthermore, the incidence of cell death was measured to determine whether differences in the rate of decrease of labelling index in the [^{3}H]thymidine pulse-chase experiment may have reflected differential rates of loss of labelled cells. Some assumptions remain untested, however, e.g. that the mitotic phase comprises a constant proportion of the cell cycle and that cell proliferation is essentially asynchronous in the cell types under study.

Role of cell proliferation in normal neurulation

Several authors have suggested mechanisms of neurulation based on neuroepithelial cell proliferation. Jelinek & Friebova (1966) observed rapid proliferation of neuroepithelial cells during neurulation in the chick. They suggested that continuing cell number increase, in a neural plate that is maintained at constant width due to tethering to the neuroepithelial basement membrane, may be directly responsible for neural folding. Smith & Schoenwolf (1987) found that localized sites of neural folding ('hinge-points') in the chick are characterized by specific neuroepithelial cell shape changes and by a longer cell cycle than in other regions of the neural plate. These authors consider that such localized differences in cell proliferation within the neuroepithelium may serve to direct the process of neural folding.

Proliferation of non-neuroepithelial cell types could also participate in the mechanism of neurulation. For instance, the development of extracellular spaces in the cranial region of rodent embryos, which have been suggested to play a direct role in the neurulation process (Morriss & Solursh, 1978), may depend on a normal rate of increase of mesodermal cell number (Marin-Padilla, 1978).

The results of the present study of neurulation in curly tail embryos provide further support for a role of cell proliferation in the mechanism of normal spinal neurulation in the mouse. Although normal proliferation of gut endoderm and notochord cells appears to be required for normal neurulation, it is not clear whether growth of these ventromedially arranged embryonic structures is the primary driving force underlying neurulation movements at the posterior neuropore or, alternatively, whether growth of gut endoderm/notochord is required in order to support morphogenesis that is driven by some other cellular event (e.g. apical microfilament contraction in neuroepithelial cells; Karfunkel, 1974). Experiments are under way to distinguish between these possible mechanisms.

Molecular basis of the cell proliferation defect in curly tail embryos

The cell-type-specific abnormality of cell proliferation in curly tail embryos could result from a molecular defect that is expressed particularly in cells of the gut endoderm and notochord. Alternatively, the molecular defect may be expressed primarily in other cell types, its effects being mediated through disturbance of a cellular interaction necessary for normal gut endoderm and notochord proliferation. Recent studies of extracellular matrix accumulation in curly tail embryos provide support for the latter hypothesis. Newly synthesized extracellular matrix hyaluronate accumulates in large amounts in the posterior neuropore region of normal mouse embryos (Copp & Bernfield, 1988*a*) whereas curly tail embryos developing spinal NTD accumulate significantly smaller quantities of hyaluronate in the posterior neuropore region (Copp & Bernfield, 1988*b*). This hyaluronate defect specifically affects basement membranes developing beneath the medial aspects of the neuroepithelium and around the notochord. Thus, the defects affecting matrix hyaluronate and cell proliferation of gut endoderm and notochord are approximately colocalized in curly tail embryos, consistent with a causal connection between the two types of abnormality. Extracellular matrices are known to promote the proliferation of cells they contact, an effect that could be mediated through the provision of a substratum to promote cell shape change (Toole, 1981), by interacting with specific cell surface matrix receptors (Horwitz *et al.* 1986) and/or by providing concentrated binding sites for growth factors (Gordon *et al.* 1987; Roberts *et al.* 1988). It is not known whether one or more of these mechanisms may operate in curly tail embryos. A further possibility, that the reduction of matrix hyaluronate is a nonspecific consequence of reduced cell proliferation in the neuropore region, also cannot be ruled out at present.

Role of cell proliferation imbalance in curly tail spinal NTD

A hypothesis arising from the findings of the present study is that spinal neural tube defects in curly tail embryos result from an imbalance of cell proliferation rates within the posterior neuropore region. That is, neuroepithelial cells proliferate normally whereas gut endoderm and notochord proliferate abnormally slowly. A test of this hypothesis is described in the accompanying paper (Copp *et al.* 1988).

We thank Professor R. L. Gardner for commenting on the manuscript. The early part of this work was performed in the Paediatric Research Unit, Guy's Hospital, London and was supported by Action Research for the Crippled

Child and the Association for Spina Bifida & Hydrocephalus. The later part of the work was supported by the Imperial Cancer Research Fund.

References

ATLAS, M. & BOND, V. P. (1965). The cell generation cycle of the eleven-day mouse embryo. *J. Cell Biol.* **26**, 19–24.

BANNIGAN, J. G. (1985). The effects of 5-bromodeoxyuridine on fusion of the cranial neural folds in the mouse embryo. *Teratology* **32**, 229–239.

COLE, W. A. & TRASLER, D. G. (1980). Gene-teratogen interaction in insulin-induced mouse exencephaly. *Teratology* **22**, 125–139.

COPP, A. J. (1978). Interaction between inner cell mass and trophectoderm of the mouse blastocyst. I. A study of cellular proliferation. *J. Embryol. exp. Morph.* **48**, 109–125.

COPP, A. J. (1985). Relationship between timing of posterior neuropore closure and development of spinal neural tube defects in mutant (curly tail) and normal mouse embryos in culture. *J. Embryol. exp. Morph.* **88**, 39–54.

COPP, A. J. & BERNFIELD, M. (1988*a*). Glycoconjugate accumulation varies along the neuraxis during spinal neurulation in the mouse embryo. *Devl Biol.* (In press).

COPP, A. J. & BERNFIELD, M. (1988*b*). Basement membrane-associated hyaluronate accumulation is reduced in the posterior neuropore region of mutant (curly tail) mouse embryos developing spinal neural tube defects. *Devl Biol.* (In press).

COPP, A. J., CROLLA, J. A. & BROOK, F. A. (1988). Prevention of spinal neural tube defects in the mouse embryo by growth retardation during neurulation. *Development* **104**, 000–000.

COPP, A. J., SELLER, M. J. & POLANI, P. E. (1982). Neural tube development in mutant (curly tail) and normal mouse embryos: the timing of posterior neuropore closure in vivo and in vitro. *J. Embryol. exp. Morph.* **69**, 151–167.

EMBURY, S., SELLER, M. J., ADINOLFI, M. & POLANI, P. E. (1979). Neural tube defects in curly tail mice. I. Incidence, expression and similarity to the human condition. *Proc. R. Soc. Lond.* B **206**, 85–94.

GILETTE, R. (1944). Cell number and cell size in the ectoderm during neurulation (Amblystoma maculatum). *J. exp. Zool.* **96**, 201–222.

GLANTZ, S. A. (1981). *Primer of Biostatistics*. New York: McGraw Hill.

GORDON, M. Y., RILEY, G. P., WATT, S. M. & GREAVES, M. F. (1987). Compartmentalization of a haematopoietic growth factor (GM-CSF) by glycosaminoglycans in the bone marrow microenvironment. *Nature, Lond.* **326**, 403–405.

GRUNEBERG, H. (1954). Genetical studies on the skeleton of the mouse. VIII. Curly tail. *J. Genet.* **52**, 52–67.

HIS, W. (1874). Unsere Korperform und des physiologische Problem ihrer Entstehung Leipzig. Cited by Holtfreter, J. (1943). *J. exp. Zool.* **94**, 261–318.

HORWITZ, A., DUGGAN, K., BUCK, C., BECKERLE, M. & BURRIDGE, K. (1986). Interaction of plasma membrane fibronectin receptor with talin – a transmembrane linkage. *Nature, Lond.* **320**, 531–533.

JELINEK, R. & FRIEBOVA, Z. (1966). Influence of mitotic activity on neurulation movements. *Nature, Lond.* **209**, 822–823.

JOHNSON, H. A. (1961). Some problems associated with the histological study of cell proliferation kinetics. *Cytologia* **26**, 32–41.

KARFUNKEL, P. (1974). The mechanism of neural tube formation. *Int. Rev. Cytol.* **38**, 245–271.

KAUFFMAN, S. L. (1968). Lengthening of the generation cycle during embryonic differentiation of the mouse neural tube. *Expl Cell Res.* **49**, 420–424.

KAUFFMAN, S. L. (1969). Cell proliferation in embryonic mouse neural tube following urethane exposure. *Devl Biol.* **20**, 146–157.

LENDON, R. L. (1972). An autoradiographic study of induced myelomeningocele. *Dev. Med. Child Neurol.* **14, Suppl. 27**, 80–86.

MARIN-PADILLA, M. (1978). Clinical and experimental rachischisis. In *Congenital Malformations of the Spine and Spinal Cord* (ed. P. J. Vinken, G. W. Bruyn & N. C. Myrianthopoulos), *Handbook of Clinical Neurology*, vol. **32**, Amsterdam: Elsevier/North-Holland Biomedical.

MORRISS, G. M. & SOLURSH, M. (1978). Regional differences in mesenchymal cell morphology and glycosaminoglycans in early neural-fold stage rat embryos. *J. Embryol. exp. Morph.* **46**, 37–52.

NEW, D. A. T., COPPOLA, P. T. & TERRY, S. (1973). Culture of explanted rat embryos in rotating tubes. *J. Reprod. Fertil.* **35**, 135–138.

PATTEN, B. M. (1953). Embryological stages in the establishing of myeloschisis with spina bifida. *Am. J. Anat.* **93**, 365–395.

PETERS, P. W. J. & DE GEUS, D. (1981). Cell proliferation of the neuroepithelium in embryonic stages of induced spina bifida. *Acta Morphol. Neerl. Scand.* **19**, 197–204.

ROBERTS, R., GALLAGHER, J., SPOONCER, E., ALLEN, T. D., BLOOMFIELD, F. & DEXTER, T. M. (1988). Heparan sulphate bound growth factors: a mechanism for stromal cell mediated haemopoiesis. *Nature, Lond.* **332**, 376–378.

SMITH, J. L. & SCHOENWOLF, G. C. (1987). Cell cycle and neuroepithelial cell shape during bending of the chick neural plate. *Anat. Rec.* **218**, 196–206.

STEEL, G. G. (1968). Cell loss from experimental tumours. *Cell Tiss. Kinet.* **1**, 193–207.

TOOLE, B. P. (1981). Glycosaminoglycans in morphogenesis. In *Cell Biology of Extracellular Matrix* (ed. E. D. Hay), pp. 259–294. New York: Plenum Press.

WILSON, D. B. (1974). Proliferation in the neural tube of the splotch (Sp) mutant mouse. *J. comp. Neurol.* **154**, 249–256.

WILSON, D. B. (1980). Cellular proliferation in the

exencephalic brain of the mouse embryo. *Brain Res.* **195**, 139–148.

WILSON, D. B. (1982). The cell cycle during closure of the neural folds in the C57BL mouse. *Develop. Brain Res.* **2**, 420–424.

WILSON, D. B. & CENTER, E. M. (1974). Neural cell cycle in the Looptail mutant of the mouse (Lp). *J. Embryol. exp. Morph.* **32**, 697–705.

WRIGHT, N. & ALISON, M. (1984). *The Biology of Epithelial Cell Populations*, vol. 2. Oxford: Clarendon Press.

(*Accepted 8 July 1988*)